

# Datasets on Energy Simulations of Standard and Optimized Buildings under Current and Future Weather Conditions across Europe

Delia D'Agostino <sup>1,\*</sup>, Danny Parker <sup>2</sup>, Ilenia Epifani <sup>3</sup>, Dru Crawley <sup>4</sup> and Linda Lawrie <sup>5</sup>

<sup>1</sup> Joint Research Centre (JRC), European Commission, 21027 Ispra, Italy

<sup>2</sup> FSEC Energy Research Center, Orlando, FL 32922, USA; dparker@fsec.ucf.edu

<sup>3</sup> Politecnico di Milano, 20133 Milan, Italy; ilenia.epifani@polimi.it

<sup>4</sup> Bentley Systems, Inc., Washington, DC 20016, USA; dbcrawley@gmail.com

<sup>5</sup> DHL Consulting, LLC, Pagosa Springs, CO 81147, USA; linda@fortlawrie.com

\* Correspondence: delia.dagostino@ec.europa.eu; Tel.: +39-033-2783512

**Abstract:** The building sector has a strategic role in the clean energy transition towards a fully decarbonized stock by mid-century. This data article investigates the use of different weather datasets in building energy simulations across Europe. It focuses on a standard performing building optimized to a nearly-zero level accounting for climate projections towards 2060. The provided data quantify the building energy performance in the current and future scenarios. The article investigates how heating and cooling loads change depending on the location and climate scenario. Hourly weather datasets frequently used in building energy simulations are analyzed to investigate how climatic conditions have changed over recent decades. The data give insight into the implications of the use of weather datasets on buildings in terms of energy consumption, efficiency measures (envelope, appliances, systems), costs, and renewable production. Due to the ongoing changing climate, basing building energy simulations and design optimization on obsolete weather data may produce inaccurate results and related building designs with an increased energy consumption in the coming decades. Energy efficiency will become more crucial in the future when cooling and overheating will have to be controlled with appropriate measures used in combination with renewable energy sources.

**Dataset:** D'Agostino, Delia; Parker, Danny; Epifani, Ilenia; Crawley, Dru; Lawrie, Linda (2022), Weather datasets and energy simulation files related to standard and optimized buildings across Europe, Mendeley Data, doi:10.17632/6krybjfsg.1, Direct URL to data <https://data.mendeley.com/drafts/6krybjfsg> (accessed on 14 April 2022).

**Dataset License:** CC-BY 4.0

**Keywords:** building design; building modeling; climate change; energy efficiency; nearly zero energy buildings (NZEBs); renewable energy; weather datasets



**Citation:** D'Agostino, D.; Parker, D.; Epifani, I.; Crawley, D.; Lawrie, L. Datasets on Energy Simulations of Standard and Optimized Buildings under Current and Future Weather Conditions across Europe. *Data* **2022**, *7*, 66. <https://doi.org/10.3390/data7050066>

Received: 15 April 2022

Accepted: 12 May 2022

Published: 14 May 2022

**Publisher's Note:** MDPI stays neutral with regard to jurisdictional claims in published maps and institutional affiliations.



**Copyright:** © 2022 by the authors. Licensee MDPI, Basel, Switzerland. This article is an open access article distributed under the terms and conditions of the Creative Commons Attribution (CC BY) license (<https://creativecommons.org/licenses/by/4.0/>).

## 1. Summary

The need for a clean energy transition reducing dependence on fossil fuels has become more urgent in the light of the recent geopolitical situation [1]. At the European level, key principles of the Green Deal are prioritizing energy efficiency, improving the energy performance of buildings, and developing a power sector based largely on renewable sources [2]. Globally, the agreed target for the coming decades is to decarbonize the energy sector, making buildings more efficient [3]. Within this framework, nearly zero energy buildings (NZEBs) have a strategic role in improving energy efficiency and renewables using a cost-optimal approach [4]. NZEBs are the mandatory target for new buildings since January 2021, as established in the Energy Performance of Building Directive [5].

A powerful way to investigate the design of NZEBs is to carry out building energy simulations with different goals, such as for the establishment of technologies [6], the prediction of energy and stock performance [7,8], the analysis of comfort and indoor air quality [9,10], the assessment of certification [11,12], and the estimation of future savings scenarios to test policy options [13,14].

Previous research by the authors determined the optimal design of NZEBs in different European climates using commonly available weather datasets [15,16]. This work showed how to reach the NZEB target with cost-optimality obtaining the best combination of efficiency measures, equipment, appliance, and renewables.

However, over the last decade, we have experienced usual and extreme weather events, especially summer heat waves [17]. At the boundary between the outdoors and indoors, it is certain that climate change will also affect buildings and occupants [18]. Nevertheless, not all the climate change effects are currently known and several possible effects need to be carefully investigated (e.g., changes in heating and cooling loads and consequent increased greenhouse gas emissions, shifts in thermal operational conditions, heating, ventilation, and air conditioning—HVAC—capacity mismatch).

Therefore, considering the climate change implications for buildings that must be properly built or renovated, it is crucial to take a forward-looking perspective [19]. Accordingly, recent research by the authors, to which the datasets of this paper refer, showed how the energy balance will be altered in European buildings in future. In more detail, heating will drop by 38–57%, while cooling will rise by +99–380% in the different tested locations [20]. Moreover, efficiency measures to reduce cooling and overheating will become more important (e.g., roof insulation, window type, solar shading, envelope finishes). Energy efficiency will have a strategic role within a changing climate scenario.

The data linked to this paper provide quantitative information on the design of NZEBs across Europe in past, present, and future climatic conditions projected to the year 2060. Currently used datasets in energy simulations can be misleading since past data drivers predict energy loads in the future. Hourly weather datasets that are frequently used in building energy simulations are provided for different locations.

The provided data account for future climate change in the simulations. These are weather morphed files for 2060 in the IPCC anticipated warming potential. We chose a 50% percentile, meaning that half of the models show a temperature offset minor or equal to that set in the scenario, with a representative concentration pathways RCP-8.5, meaning that an additional radiation of  $8.5 \text{ W/m}^2$  is foreseen towards the year 2100 [21–24]. The linked data emphasize an all-electric residential building prototype modeled to investigate how climate change will impact buildings in terms of design, efficiency measures, loads, and renewable production.

The purpose of this paper is to provide data and methods on how climate change may also impact the design of NZEBs, heating and cooling loads, the selection of cost-optimal energy efficiency measures, and the production of renewable energy in different European climates. The target stakeholders of this paper and related dataset are mainly related to the scientific and policy community dealing with buildings and energy. The potential benefits are huge considering how the selection of weather datasets is crucial in modeling [25–27]. Another benefit is the support to EU policies related to technologies to be favored in buildings, energy performance calculations, design trends of NZEBs, and climate change impact on future buildings. The impact of the paper relates to the inclusion of climate change projections to predict the long-term performance and optimization of NZEB design. This inclusion considerably changes the energy balance in buildings and the efficiency measures needed to reduce cooling needs and overheating. Climatic parameters have evolved considerably over recent decades, and past weather datasets should not be used in order to avoid unreliable simulation results. A major finding is that improving energy efficiency will be even more crucial within a climate change scenario.

## 2. Data Description

The shared datasets include both the weather datasets and the building simulations files that can be used to investigate the impact of climate on energy performance and NZEB design as comprehensively illustrated in [20]. Eight locations are included in the datasets:

- Stockholm (Sweden)
- Milan (Italy)
- Vienna (Austria)
- Madrid (Spain)
- Paris (France)
- Munich (Germany)
- Lisbon (Portugal)
- Rome (Italy)

The locations were selected to have a good coverage of the European climatic variability based on heating and cooling degree days. The hourly files used in building energy simulations are available.

Yearly weather datasets (lsx) were collected and analyzed from 2003 to 2018 (folder “hourlyWeatherDatasets”). The folder contains the hourly weather datasets for all locations, heating and cooling loads (detailed per use) in: 2003, 2004, 2005, 2006, 2007, 2008, 2009, 2010, 2011, 2012, 2013, 2014, 2015, 2020, 2017, 2018, 2018 TMY (typical metrological year), IWEC (International Weather for Energy Calculations), IWEC2, 2060. Sensitivity analysis is available for Milan and Stockholm.

In more detail, in the analysis, IWEC and TMY datasets were included as they are commonly used in building simulations. The IWEC and IWEC2 hourly datasets refer to the average weather observed, or TMY, over the last 15–25 years (IWEC 1984–2001, IWEC2 1994–2011) [28–30]. Single years are able to give the tendency of the ongoing conditions [31,32]. More recent TMYs are currently also available [33], together with data collected since 2011 based on satellite data [34].

In order to include climate change and obtain the 2060 projection, we considered the IPCC 5th assessment applying a down-scaling methodology to the most recent TMY file (2004–2018) [21–35]. The method is summarized in [36]. We referred to the commercially available Weather-Shift implementation of the Belcher et al. calculation [21]. We selected a business-as-usual scenario with limited mitigation (RCP 8.5 median 50%) including a sensitivity analysis of 10% and 90% lower and upper bound cases [37,38].

The shared datasets also relate to the building simulation files and related outputs in different climates. The data were elaborated using the open source tool BEopt [39]. BEopt is powered by the EnergyPlus and TRNSYS simulation engines. The first derives hourly heating, cooling, water heating, and appliance loads. The second estimates the renewable production for photovoltaic electric and solar water heating. Starting from the standard configuration, a sequential search technique is used to optimize the design. This allows calculation of the annual loads and resulting costs. The methodology, characteristics of the standard building, and assumptions are set out fully in [20].

The shared data allow us to identify, starting from a standard building, the optimal building design to reach NZEBs at the lowest cost in different climates. The data provide information on efficiency measures, envelope characteristics, equipment and systems, lighting, renewables, and costs in new residential buildings, both in current and future climate scenarios. The data include energy consumption, energy savings, and implemented measures in the base and optimized configurations.

The folder “building simulation file” contains the Beopt (.BEopt) and EnergyPlus (epw) files for the standard and optimized buildings in all locations, with present and future climates, the IDF (input data file), and XML executable files. The XML file provides data mapping between EnergyPlus and the external interface. The appliance schedules for the hourly simulation are contained in 1\_sched.csv. The domestic hot water (DHW) schedules and quantities are contained in the DHW\_3bed\_unit0\_10 min.csv file.

The folder “simulation file outputs” contains the annual simulation file results for all the studied locations and weather datasets. Heating and cooling loads (detailed per use) are given for: 2003, 2004, 2005, 2006, 2007, 2008, 2009, 2010, 2011, 2012, 2013, 2014, 2015, 2020, 2017, 2018, 2018 TMY, IWEC2, IWEC, 2060. The variances from the 15-year average and weather averages are also given.

The subfolder “Standard and Optimized building\_outputs\_2018TMY and the 2060TMY” details the results (e.g., simulated electrical end-uses in kWh for: miscellaneous, ventilation fan, appliances, lights, cooling fan/pump, heating fan/pump, cooling, heating, hot water, total, PV, net) for all locations in terms of standard and optimized buildings using the TMY 2018 and TMY 2060 weather datasets.

The heating system comprises an air source heat pump so that there is energy use for the indoor fan blower, the outdoor compressor, and supplemental (Suppl.) heat which uses resistance heat when outdoor temperatures are very low and the compressor no longer has sufficient capacity for heating. An important part of the study is the consideration of PV changes in a climate change scenario. Forecasts indicate a warmer climate and a reduction in prevailing clouds. Furthermore, on-site short-term electrical storage systems are also considered for the first time as projections indicate that this system will be widely available and increasingly affordable in coming decades.

### 3. Methods

Comprehensive weather datasets are given in the provided data as detailed in Section 2. A preliminary analysis of the weather datasets was carried out to check for missing data and make relative corrections.

The weather data for Milan are 403K hourly data points (e.g., dry and wet bulb temperature, dew-point, relative humidity, wind direction and speed, global and diffuse horizontal radiation, precipitation, and sky cover) from 1973 to 2020. The average, variance, standard deviation, maximum, and minimum can be visualized as boxplots to show the distribution of the climatic variables using dispersion and position indexes.

As a data visualization example, Figure 1 shows the temperature and monthly boxplots, while Figure 2 shows the temperature boxplot, medians, and inter-quartile binned over five years from 1973 to 2018.

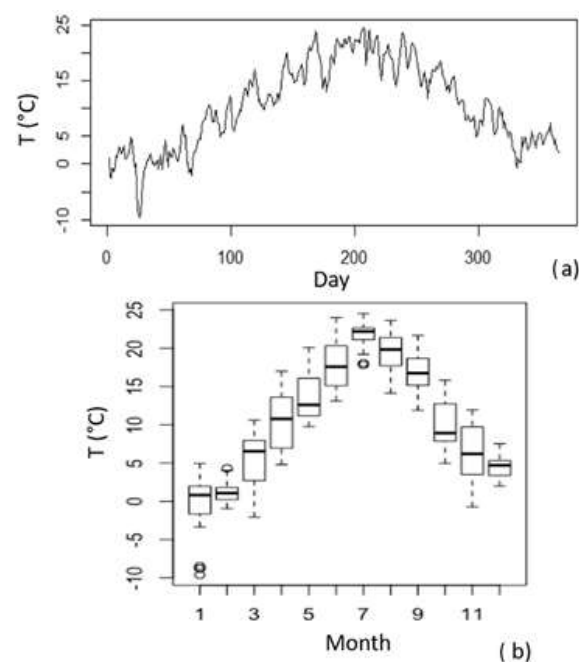


**Figure 1.** (a) Temperature in 2000; (b) boxplot of monthly temperature in 2000 (Milan).



Table 1 confirms that the variables related to irradiance (in red) are strongly related to each other and to temperature.

Other statistical methods applied on weather datasets, temperature, and buildings' performance variation are reported in Appendix A.

To evaluate the building design in current and future climates, a simulation-based optimization model is developed as described in [20]. A standard residential building prototype has been optimized to NZEBs to derive the most cost-effective design.

The methodology followed to produce the data includes a consideration of climate change both in the model set-up and in the weather datasets used to carry out the energy simulations. Among the important novelties:

- the building is all-electric, in line with the EU strategy of a future electrification of the sector;
- an updated library of energy efficient options (envelope, appliances, systems) is included, in particular the building envelope generally has a long-term impact due to the differing lifetime time horizon;
- the cooling set points are set upwards to 25.6 °C for the control air node operative temperature in compliance with ISO Standard 7730;
- a standard air-source heat pump is selected with electric resistance and a seasonal coefficient of performance (SCOP = 2.4) evaluated at multiple temperature conditions in EN 14511 and EN 14825. The operating SCOP varies depending on both the prevailing temperature conditions and building characteristics;
- a more efficient heat pump (SCOP = 3.1) is also available. This system is often selected, particularly in extreme heating or cooling climates.

We improve the standard building to reach the NZEB target (90% reduction in primary energy) at the lowest possible cost in specific locations.

Once the model has evaluated the standard building performance, all options are compared in a series of parametric evaluations, as reported in (1).

$$ESavings_{i,n} = (\text{Base energy}_n - \text{Measure energy}_{n,i}) \quad (1)$$

where:

$ESaving_{n,i}$  = energy savings within optimization iteration 'n' evaluated for option 'i'.

$\text{Base energy}_n$  = calculated energy use of the standard building at the beginning of iteration 'n'.

$\text{Measure energy}_{n,i}$  = estimated energy use of the base building with measure 'i' installed within iteration 'n'.

The optimal range is assessed, analysing the primary energy and global costs related to the tested measures. The lowest point of the curve that belongs to the band is indicative of the optimal configuration [40–42]. The total costs over the life are then annualized to an annual cost of energy and additional mortgage linked to the added incremental costs [43].

At each iteration, the single most cost-effective option (lowest annualized cost of investment and energy costs) is selected after having evaluated all measures. Within the optimization process, the standard building evolves, and it is modified by adding the selected option at the end of an iteration before proceeding to the next. All remaining options are then re-evaluated together with the next selected option. This process continues until the performance target is reached, until zero energy is achieved using renewables, or the available cost-effective options are exhausted (Figure 4).

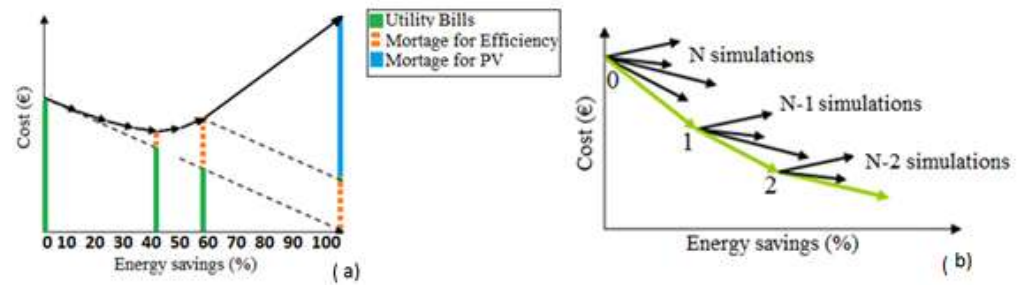


**Figure 4.** (a) Evaluation method; (b) the sequential search process for NZEBs (source: [15]).

The sequential search technique allows us to reach the established target locating the least expensive path. It also locates intermediate optimal points. Thus, it is possible to identify what the 50% reduction level is along the path to reach a NZEB target.

For each location, the software ran around 200–400 simulations in 15–25 iterations to reach the target. A total of 19 weather datasets (e.g., IWEC, IWEC2, TMY, yearly datasets from 2003 to 2018, TMYshift\_2060) were included for all locations (152 simulations for the standard building).

Global costs ( $C_G$ ), in terms of net present value (NPV), for each combination of measures are derived using UNI EN 15459 [44].

The cost-effectiveness of each option is derived by estimating the NPV of the cost of the improvement or change over the life of the building. This is compared with the cost of the changing standard building:

$$\text{NPV}_{n,i} = I(V_n a^n) \quad (2)$$

$$\text{PV} = I(V_n a^n) + \sum_{j=1}^n a^j (M_j + R_j) + \sum_{k=1}^H \sum_{j=1}^n P_k Q_k b^j \quad (3)$$

where:

PV = total present-value of life-cycle costs before taxes;

I = total first costs associated with energy saving measure;

$V_n$  = residual or salvage value at year  $n$ , the last year in the evaluation (50 years);

$a$  = single-present-value formula from  $j = 1$  to  $n$ , and discount rate  $d$ ; i.e.,  $a^j = (1 + d)^{-j}$ ;

$M_j$  = maintenance costs in year  $j$ ;

$R_j$  = repair and replacement costs in year  $j$ ;

$P_k$  = the initial price of the  $k$ th type of conventional energy carrier for energy types  $k = 1$  to  $H$ ;

$Q_k$  = the quantity required of the  $k$ th type of energy;

$b^j$  = a formula for finding the present value of an amount in the  $j$ th year, escalated at a rate  $\Theta_k$ , where  $k$  denotes the  $k$ th type of energy carrier, and discounted at a rate  $d$ ; i.e.,  $b^j = [(1 + \Theta_k)/(1 + d)]^j$ .

The costs related to building elements not influencing the energy performance are omitted. The calculation considered an initial investment  $C_I$  and a yearly cost for every year  $i$  (referred to the starting year) for each component or system  $j$ , and a final value. Global cost ( $C_G$ ) takes into account the calculation period  $\tau$  according to (4):

$$C_G(\tau) = C_I + \sum_j \left[ \sum_{i=1}^{\tau} (C_{a,i}(j) \times R_d(i)) - V_{f,\tau}(j) \right] \quad (4)$$

The final value  $V_{f,\tau}(j)$  of a component is found by a straight-line depreciation of the initial investment until the calculation period end in reference to the start. If the calculation

period  $\tau$  exceeds the lifespan  $\tau_n(j)$  of the considered component ( $j$ ), the last replacement cost is accounted for in the straight-line depreciation as:

$$V_{f,\tau}(j) = V_0(j) \times (1 + R_p/100)^{n_{\tau}(j) * \tau_n(j)} \times \left[ \frac{(n_{\tau}(j) + 1 \times \tau_n(j) - \tau)}{\tau_n(j)} \right] \times R_d(\tau) \quad (5)$$

where:

$$V_0(j) \times (1 + R_p/100)^{n_{\tau}(j) * \tau_n(j)} \quad (6)$$

is the last replacement cost, when considering the development rate of the price for products ( $R_p$ );

$$\frac{(n_{\tau}(j) + 1 \times \tau_n(j) - \tau)}{\tau_n(j)} \quad (7)$$

is the straight-line depreciation of the last replacement cost;

$$R_d(\tau) = \left( \frac{1}{1 + R_R/100} \right) \quad (8)$$

$i$  the discount rate at the end of the calculation period, and the real interest rate, depending on the market interest rate  $R$  and on the inflation rate  $R_i$ .

In relation to the economic parameters, the cost-effectiveness calculations of individual measures are based on the present value of life-cycle costs considering projections over 30 years. The methodologies for life-cycle calculations are in [45,46].

The assumed costs, service lives, and maintenance fractions for each of the hundreds of efficiency measures considered are given in an Excel sheet linked to the simulation. They are based on recommended guidelines supplementing Directive 2010/31/EU [4]. The energy costs for electricity are taken from [47,48].

No financial incentives have been assumed for either efficiency or renewable energy sources. However, a differing lifetime is specified for each measure considering data from a number of sources, including Standard EN-15459 [44].

The energy price inflation rate approximates the EU Emissions Trading Scheme with carbon pricing of 25 EUR/tCO<sub>2</sub> in 2020 to 39 EUR/tCO<sub>2</sub> in 2020. It is possible to alter the input parameters to consider very long time horizons and/or higher energy inflation rates. The optimization can also be limited to non-equipment options, providing a better evaluation of one-time interventions, such as those related to envelope insulation [49,50].

In relation to the modeled building, the data include an updated library of energy efficient options [51,52]. This includes technical data, climate, energy parameters, operation, maintenance, and replacement costs of measures related to the envelope, appliances, and systems [53,54].

The provided data include model inputs and outputs [55,56] (Figure 5).

The cost-optimal curve showing global costs (EUR/m<sup>2</sup>) and energy consumption (kWh/m<sup>2</sup>y) can be visualized [57,58]. The outputs can be graphed to show energy consumption, savings, selected efficiency measures, costs, and renewable production in present and future climates, before and after the optimization, and in current and future conditions [59].

Examples of data visualization from the provided dataset are shown in Figures 6 and 7 in relation to Rome and Stockholm (data available from the folder “simulationFilesOutputs”). The figures show how climate change impacts the balance of heating and cooling in buildings in Rome and Stockholm from 2018 to 2060. The results also show how NZEB efficiency improvements help to control these differences.



<b>Building</b> EPW Location: ITA_LZ_Rome-Fiumicino.Da.Vinci.a Terrain: Suburban Natural Gas Hookup: <input checked="" type="checkbox"/>		<b>Mortgage</b> Down Payment: 10.0 % Mortgage Interest Rate: 5.0 % Mortgage Period: 30 years Marginal Income Tax Rate, Federal: 0.0 % Marginal Income Tax Rate, State: 0.0 %	
<b>Economics</b> Project Analysis Period: 30 years Inflation Rate: 2.0 % Discount Rate (Real): 5.0 % Efficiency Material Cost Multiplier: 1.000 Efficiency Labor Cost Multiplier: 1.000 PV Material Cost Multiplier: 0.655 PV Labor Cost Multiplier: 0.655		<b>Other</b> Incentives: <input checked="" type="checkbox"/> PV Efficiency (Whole-Building) Demand Response: Signals	
<b>Electricity</b>   Natural Gas   Oil   Propane			
<b>Utility Rates</b> <input checked="" type="radio"/> Simple <input type="radio"/> Detailed <input checked="" type="radio"/> User Specified <input type="radio"/> State Average <input type="radio"/> National Average Fixed: 0.00 \$/month Marginal: 0.2300 \$/kWh Average: 0.2300 \$/kWh Fuel Escalation (Real): 1.00 %/year		<b>PV Compensation</b> <input checked="" type="radio"/> Net Metering <input type="radio"/> Feed-in Tariff Annual Excess Sellback Rate <input checked="" type="radio"/> Retail Electricity Cost: 0.23000 \$/kWh <input type="radio"/> User Specified Monthly Grid Connection Fee: 0.00 \$/kW	
		<b>Energy Factors</b> Source/Site Ratio: 2.000 Carbon Factor: 1.077 lb/kWh	

Figure 5. Data model input parameters.

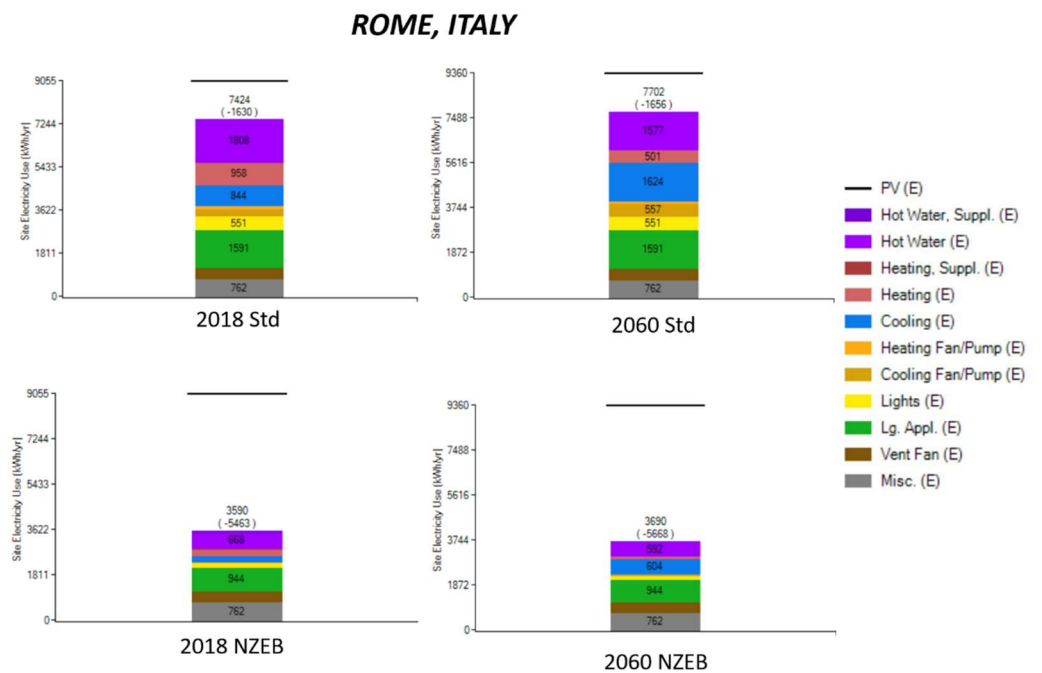
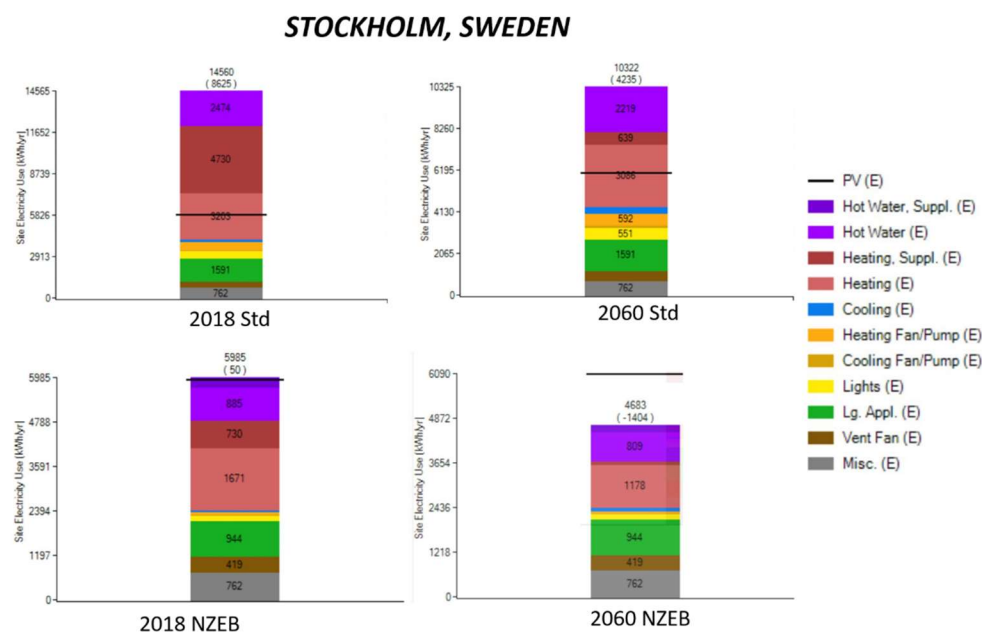


Figure 6. Data processed for the Milan case in 2018 and in 2060 (climate change scenario). The site electricity use is shown for the standard (Std) and optimized building (NZEB). Raw data provided within the datasets.



**Figure 7.** Data processed for Stockholm in 2018 and in 2060 (climate change scenario). The site electricity use is shown for the standard (Std) and optimized building (NZEB). Raw data provided within the datasets.

Table 2 shows the outputs for the building located in Milan for the TMY2018 weather file with a standard (Std) building.

**Table 2.** Standard building performance in Milan for the TMY2018 weather dataset (E = electricity). Raw data provided within the datasets.

End Use	Annual kWh
Misc. (E)	762.0
Vent Fan (E)	454.3
Lg. Appl. (E)	1591.5
Lights (E)	551
Cooling Fan/Pump (E)	187.6
Heating Fan/Pump (E)	442.6
Cooling (E)	524.6
Heating (E)	2230.4
Heating, Suppl. (E)	381.1
Hot Water (E)	2086.8
Total	9212
PV	7623
Net (Total PV)	1589

The simulation outputs show different results in the energy uses of the building prototype and different optimization results of the selected energy efficiency measures in the studied locations which are due to the changed climate data [60,61]. This dataset does take climate change into account, and this is evident in the altered building loads and, in particular, in the increased cooling needs of the residential prototype [62]. The selected options differ in many cases based on the altered weight of heating and cooling based on the morphed climate files. It is possible to visualize the selection of main efficiency options related to: building orientation, walls, ceilings, roofs, foundation, thermal mass, windows, airflow, and space conditioning. Different technical and cost data have been defined and are available within the provided files.

**Author Contributions:** Conceptualization, D.D. and D.P.; methodology, D.D. and D.P.; software, D.D. and D.P.; validation, D.D. and D.P.; formal analysis, D.D. and D.P.; investigation, D.D. and D.P.; datasets providers, D.C. and L.L.; data curation, D.D., D.P. and I.E.; writing—original draft preparation, D.D. and D.P.; writing—review and editing, D.D., I.E. and D.P.; visualization, D.D. and D.P.; supervision, I.E. All authors have read and agreed to the published version of the manuscript.

**Funding:** This research received no external funding. This effort did not receive any specific grant from funding agencies in the public, commercial, or not-for-profit sectors.

**Informed Consent Statement:** Not applicable.

**Data Availability Statement:** Data available in a publicly accessible repository. The data presented in this study are openly available in Mendeley Data at doi:10.17632/6krybfjfg.1, <https://data.mendeley.com/datasets/6krybfjfg/draft?a=78f46cfb-c887-4604-95bb-e9d5c7cebd10> (accessed on 14 April 2022).

**Acknowledgments:** We appreciate the support of Christian Thiel and Maurizio Bavetta at the Joint Research Centre (European Commission, Ispra, Italy) and James Fenton (University of Central Florida/FSEC Energy Research Center) in encouraging this collaborative research. The authors thank Diana Bernasconi, Alice Fabbretto, Matteo Eritrei, Irene Pincolini, and Rossella Venturella that were part of the preliminary project shown in Appendix A. The outputs of this analysis laid the basis for the further investigations that gave rise to this topics developed in the paper.

**Conflicts of Interest:** The authors declare no conflict of interest.

## Appendix A

Temperature can be analyzed as a historical series, considering representative years. The analysis of time series is aimed at understanding phenomena that evolve over time in a non-deterministic way. A time series (or historical series) can be thought of as the realization of the sum of a systematic (or deterministic) part and a random part (error), and regression techniques are used to investigate them. The deterministic component is broken down into three components: trend, cyclicity, and seasonality. Anything not explained by the deterministic part is considered a random residual. The two main models of this approach are the additive and multiplicative models in Equation (1):

$$Y_t = T_t + C_t + S_t + E_t \quad \text{or} \quad Y_t = T_t * C_t * S_t * E_t, \quad t = 1, \dots, T$$

Alternatively, the time series can be seen as a realization of a stochastic process,  $Y = \{Y_t, t \in T\}$  and, a particular sequence generated by the process is its trajectory (or realization). Data can then be used to derive the probabilistic law (or some of its aspects) of the stochastic process that generated them, that is, to trace the analysis of time series to a problem of statistical inference on stochastic processes. Here, an ARIMA (autoregressive integrated moving average) process has been used to fit the temperature series and give predictions.

A trajectory  $y = \{y_t, t \in T\}$  is said to be generated by an autoregressive moving average process,  $Y = \{Y_t, t \in T\}$  of order  $(p, q)$  (ARMA $(p, q)$ ) when generated by the following difference equation:

$$y_t = \eta + \phi_1(y_{t-1} - \eta) + \dots + \phi_p(y_{t-p} - \eta) + u_t + \theta_1 u_{t-1} + \dots + \theta_q u_{t-q} \quad (\text{A1})$$

In Equation (A1) AR component  $\phi_1(y_{t-1} - \eta) + \dots + \phi_p(y_{t-p} - \eta)$  is a linear regression of the variable on its lagged-time values. The MA component  $u_t + \theta_1 u_{t-1} + \dots + \theta_q u_{t-q}$  is also a linear model whose regressors are the errors in the prediction of the previous  $q$  terms. If series  $Y$  is non-stationary, the non-stationary component can be modeled by adding the integrated part to the previously defined ARMA model (A1):

$$(1 - B)^d y_t = z_t \quad \text{with} \quad \phi(B)(z_t - \eta) = \vartheta(B)$$

where  $B$  is the lag operator:  $B^d y_t = y_{t-d}$ . In this case, the reference is an integrated moving average self-regressive model of order  $(p, d, q)$ : ARIMA $(p, d, q)$ .

The model orders  $p, d, q$  were defined by analyzing the partial autocorrelation and autocorrelation function for  $q$  and  $p$ , and “counting” the differentiations required to make the series stationary for  $d$ .

The ACF autocorrelation function is calculated as:

$$\rho(y_t, y_{t+k}) = \frac{\text{cov}(y_t, y_{t+k})}{\sigma_t \sigma_{t+k}}$$

Instead, the PACF partial autocorrelation function measures the link between the  $y_t$  and  $y_{t+k}$  variables net of the influence exerted by intermediate variables.

The ARIMA results are shown in terms of the autocorrelation function, separately for 2000, 2010, and 2020 in Figure A1. The temperature series are positively correlated during winter and early spring, negatively in summer, and again positively in the following autumn and winter, which is also what is expected given the presence of seasonality (Figure A1).

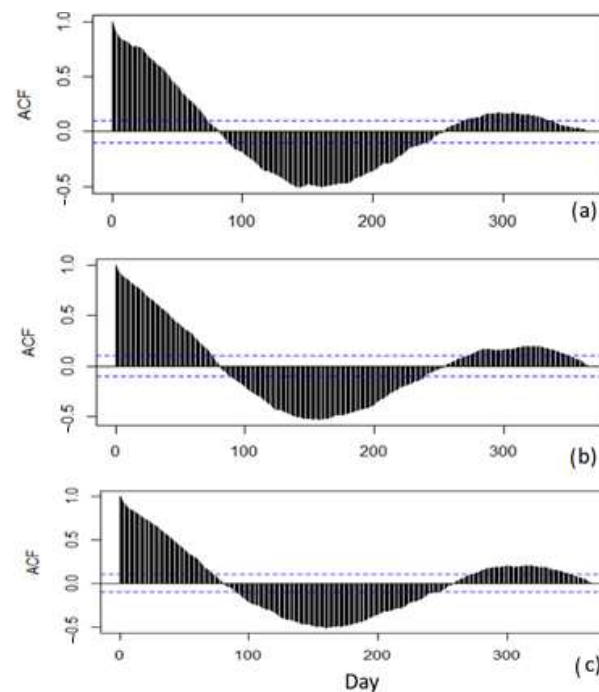


**Figure A1.** Autocorrelation function in (a) 2000, (b) 2010, (c) 2020.

The stationary nature of the series can be examined: as is evident from Figure A1, the temperature is not stationary. By differentiate the series, the deterministic trend and seasonability are no longer evident, and the resulting series can be considered stationary. To derive the  $p$  and  $q$  parameters, the autocorrelation and partial autocorrelation of the stationary series were analyzed: there is total autocorrelation at time 1 so  $q = 1$  and partial autocorrelation to time 2, then  $p = 2$ . The reference model to be used is therefore an ARIMA(2,1,1); this result is obtained by the R software through the `autoarima` function that provided the ARIMA model that best fits the data according to the lowest value of AIC.

For each of three years, an ARIMA(2,1,1) was chosen as the best ARIMA random process, indicating the homogeneity of the three series. However, this does not imply no change occurring: the effect of climate change is usually evident on a larger time scale. The closeness between the years can therefore be considered as the reason for this similarity.

The least squares method was implemented for the parameters estimation in R software (with `ts` package). The values of the model coefficients and their standard errors are shown in Table A1.

**Table A1.** Coefficients of the ARIMA model and standard errors.

	AR1	AR2	MA1	AIC
2000	1.0142	−0.202	−0.8887	1341.99
	0.0606	0.0519	0.0368	
2010	0.7496	−0.2915	−0.6754	1298.5
	0.1249	0.0536	0.1292	
2020	0.9577	−0.2327	−0.8307	1279.53
	0.0773	0.0518	0.0632	

To verify the model estimation, residuals were analyzed:

$$\varepsilon_t = y_t - \hat{y}_t$$

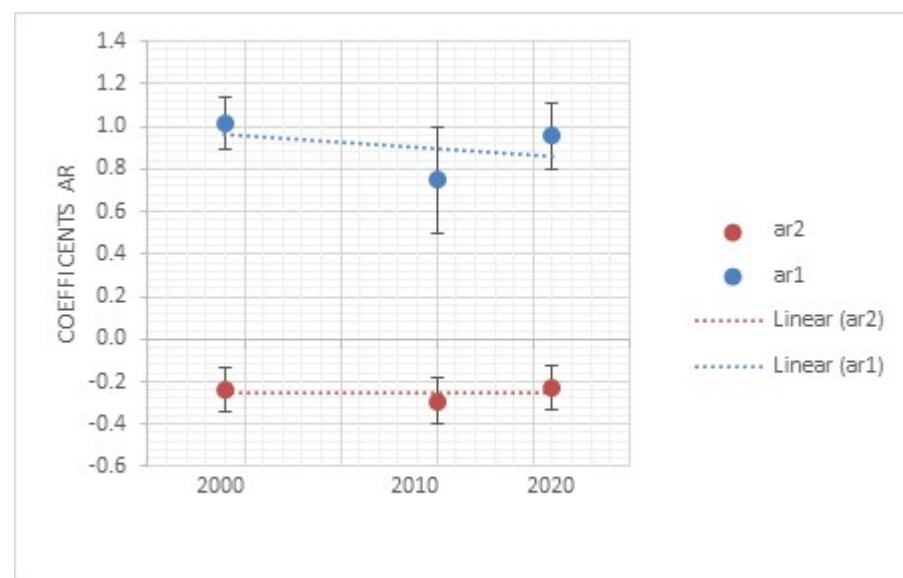
If the historical series are correctly represented by the ARIMA model, then the estimated residuals should not have a linear dependency, i.e., simple, and partial self-correlations should be of low significance.

To check for the absence of autocorrelation we use the test statistic  $LB$  in Equation (A2) that is an appropriate linear combination of the autocorrelation coefficients of the residuals  $r(t)$ :

$$LB = n(n+2) \sum_{t=1}^k \frac{r^2(t)}{n-t} \quad (A2)$$

where  $k$  is the maximum delay of significantly different self-correlations. After  $k$ , a stationary random process should make all self-correlations zero. If the null hypothesis (absence of autocorrelation) is true, the test statistic  $LB$  is asymptotically chi squared-distributed with  $k$  degrees of freedom. Tests exhibit very high values of the  $p$ -values (0.9 for 2000 and 2010, and 0.6 in 2020), then we concluded there is no correlation between the residuals.

The difference in the values of the estimated coefficients could indicate a change in temperatures: to analyze this possibility, confidence intervals of two autoregressive parameters at 97.5% level in 2000, 2010, and 2020 were used. They are graphically reported in Figure A2.

**Figure A2.** Confidence intervals.

The graphs in Figure A2 show the variability between years with regard to the AR(2) coefficient. In the AR(1) coefficient, there is a decreasing trend of values over time which consists of a decrease in system memory.

The relation between temperature variations and the building's performance, in particular on heating and cooling loads, was also investigated. The standard and the optimized buildings were compared using hourly data of heating and cooling [KWh] (the boxplot in Figure A3 shows the seasonality of both loads).

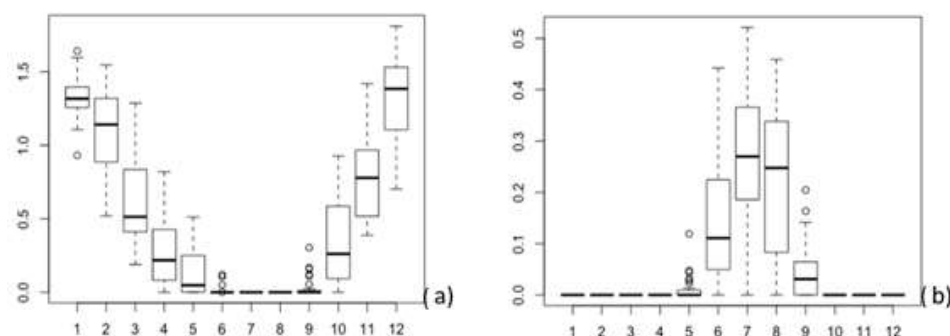


Figure A3. Boxplot (a) heating, (b) cooling (2000).

The following building types were identified by the Tabula project [40]:

- Building 1: single-family house, characterized by a single real estate unit of an isolated type of one or two floors;
- Building 2: terraced house, characterized by a single real estate unit of one or two floors neighboring other housing units;
- Building 3: multi-family building characterized by a limited number of real estate units, from two to five floors and up to 15 apartments.
- Building 4: block of apartments, large building characterized by a higher number of real estate units.



Figure A4. Buildings identified by the Tabula project in reference to the climatic area of interest. Archetypes are illustrated through a real image and simplified volumetric sketch.

The interactions between years and buildings were studied applying a statistical comparison test for each building over years (year effect), and for each year on all buildings (building effect); a significance level of 5% has been used. The statistical tests were performed on the standard buildings for both heating and cooling, then for the optimized buildings, finally the results were compared to each other. As the data are neither Gaussian, nor homoscedastic, instead of ANOVA (analysis of variance) analysis, the non-parametric (global) Kruskal-Wallis test was carried out with the non-parametric post hoc pairwise Wilcoxon rank sum tests (making a comparison in pairs); Table A2 shows  $p$ -value of the tests.

**Table A2.** *p*-value of Kruskal–Wallis test and pairwise Wilcoxon rank sum test.

Standard	Heating		Cooling	
	Building effect	<i>p</i> -value	Test	<i>p</i> -value
2000	0.0027	Building 4	0	Building 3, Building 4
2010	0.0006	Building 3 Building 4	0	No-sign. difference
2020	0.0101	Building 4	0	No-sign. difference
Year effect				
Building 1	0.0086	2000–2020	0.0979	No-sign. difference
Building 2	0.0061	2000–2020	0.0015	2000
Building 3	0.0177	2000–2020	0.0135	2020
Building 4	0.0082	2000–2020	0.0016	2020
<b>NZEBs</b>				
Building effect	<i>p</i> -value		<i>p</i> -value	
2000	0	Building 1	0.5595	No-sign. difference
2010	0.1760	Building 2	0.8892	No-sign. difference
2020	0.1760	Building 2	0.8892	2020
Year effect				
Building 1	0.1922	2020	0.9794	No-sign. difference
Building 2	0.0177	2020	0.9609	No-sign. difference
Building 3	0.6468	2020	0.9901	No-sign. difference
Building 4	0.4642	2020	0.9990	No-sign. difference

There was variability in the response both for the building type and the years under consideration. In the optimized buildings, there were variations only in heating and in particular for 2020 and Building 2. The results of the test show that Buildings 2 and 4 are the most sensitive types to climatic variability, one for cooling (high external temperatures) and one for heating (low external temperatures). In addition, there was a change in the behavior of buildings among years: between 2000 and 2020 for heating and 2020 compared to the other two years for cooling, which could be due to temperatures changes. After this preliminary analysis, Building 1 was selected for further investigations as reported in the paper. With the building optimization, both “the building effect” and the “year effect” are almost completely absorbed. This change in behavior confirms that the design of buildings is crucial for a lower sensitivity to climatic variations, in particular to reduce heating and cooling loads.

## References

1. EC, REPowerEU: Joint European Action for More Affordable, Secure and Sustainable Energy. March 2022. Available online: [https://ec.europa.eu/commission/presscorner/detail/en/fs\\_22\\_1938](https://ec.europa.eu/commission/presscorner/detail/en/fs_22_1938) (accessed on 14 April 2022).
2. EC, the European Green Deal, COM (2019) 640 Final, Communication from the Commission to the European Parliament, the European Council, the Council, The European Economic and Social Committee and the Committee of the Regions. Available online: [https://ec.europa.eu/info/sites/info/files/european-green-deal-communication\\_en.pdf](https://ec.europa.eu/info/sites/info/files/european-green-deal-communication_en.pdf) (accessed on 29 March 2022).
3. Economidou, M.; Todeschi, V.; Bertoldi, P.; D'Agostino, D.; Zangheri, P.; Castellazzi, L. Review of 50 years of EU energy efficiency policies for buildings. *Energy Build.* **2020**, *225*, 110322. [[CrossRef](#)]
4. EU. Directive 2010/31/EU. European parliament and of the council of 19 May 2010 on the energy performance of buildings (recast). *Off J. Eur. Union* **2010**, L 153/13. Available online: <https://eur-lex.europa.eu/legal-content/EN/TXT/PDF/?uri=CELEX:32010L0031&from=EN> (accessed on 29 March 2022).
5. Revision of the Directive of the European Parliament and of the Council on the Energy Performance of Buildings (Recast), COM(2021) 802 Final. Available online: <https://ec.europa.eu/energy/sites/default/files/proposal-recast-energy-performance-buildings-directive.pdf> (accessed on 10 March 2022).
6. Gaterell, M.R.; McEvoy, M.E. The impact of climate change uncertainties on the performance of energy efficiency measures applied to dwellings. *Energy Build.* **2005**, *37*, 982–995. [[CrossRef](#)]
7. Herrera, M.; Natarajan, S.; Coley, D. A review of current and future weather data for building simulation. *J. Build. Serv. Eng. Res. Technol.* **2017**, *38*, 602–627. [[CrossRef](#)]
8. Bot, K.; Ramos Nuno, M.M.; Almeida, R.M.S.F.; Pereira, P.F.; Monteiro, C. EO with on-site energy generation and storage—An integrated assessment using dynamic simulation. *J. Build. Eng.* **2019**, *24*, 100769. [[CrossRef](#)]
9. Roberts, M.; Allen, S.; Coley, D. Life cycle assessment in the building design process—A systematic literature review. *Build. Environ.* **2020**, *185*, 107274. [[CrossRef](#)]
10. Ferrara, M.; Fabrizio, E.; Virgone, J.; Filippi, M. A simulation based optimization method for cost-optimal analysis. *Energy Build.* **2014**, *84*, 442–457. [[CrossRef](#)]
11. Österbring, M.; Mata, É.; Thuvander, L.; Mangold, M.; Johnsson, F.; Wallbaum, H. A differentiated description of building-stocks for a georeferenced urban bottom-up building-stock model. *Energy Build.* **2020**, *120*, 78–84. [[CrossRef](#)]
12. Ganesh, H.S.; Seo, K.; Fritz, H.E.; Edgar, T.F.; Novoselac, A.; Baldea, M. Indoor air quality and energy management in buildings using combined moving horizon estimation and model predictive control. *J. Build. Eng.* **2021**, *33*, 101552. [[CrossRef](#)]
13. Jeong, J.; Hong, T.; Ji, C.; Kim, J.; Lee, M.; Jeong, K.; Koo, C. Development of a prediction model for the cost saving potentials in implementing the building energy efficiency rating certification. *Appl. Energy* **2007**, *189*, 257–270. [[CrossRef](#)]
14. Nägeli, C.; Jakob, M.; Catenazzi, G.; Ostermeyer, Y. Policies to decarbonize the Swiss residential building stock: An agent-based building stock modeling assessment. *Energy Policy* **2020**, *146*, 111814. [[CrossRef](#)]
15. D'Agostino, D.; Parker, D. A framework for the cost-optimal design of nearly zero energy buildings (NZEBs) in representative climates across Europe. *Energy* **2018**, *149*, 814–829. [[CrossRef](#)]
16. D'Agostino, D.; Parker, D. Data on cost-optimal Nearly Zero Energy Buildings (NZEBs) across Europe. *Data Brief* **2018**, *17*, 1168–1174. [[CrossRef](#)] [[PubMed](#)]
17. Solomon, S. *Climate Change 2007: The Physical Science Basis*; Cambridge University Press: Cambridge, UK, 2007.
18. Guan, L. Preparation of future weather data to study the impact of climate change on buildings. *Build. Environ.* **2009**, *44*, 793–800. [[CrossRef](#)]
19. Robert, A.; Kummert, M. Designing Net Zero Energy Buildings for the Future Climate, not for the Past. *Build. Environ.* **2012**, *55*, 150–158. [[CrossRef](#)]
20. D'Agostino, D.; Parker, D.; Epifani, I.; Crawley, D.; Lawrie, L. How will future climate impact the design and performance of Nearly Zero Energy Buildings (NZEBs)? *Energy* **2022**, *240*, 122479. [[CrossRef](#)]
21. Belcher, S.E.; Hacker, J.N.; Powell, D.S. Constructing design weather data for future climates. *Build. Serv. Eng. Res. Technol.* **2005**, *26*, 49–61. [[CrossRef](#)]
22. UNFCCC. Adoption of the Paris Agreement. Proposal by the President. In Proceedings of the Paris Climate Change Conference, Paris, France, 30 November–12 December 2015.
23. IPCC. *Climate Change 2014: Synthesis Report, 5th Assessment Report of the Intergovernmental Panel on Climate Change*; Pachauri, R.K., Meyer, I.A., Eds.; IPCC: Geneva, Switzerland, 2014.
24. Schwalm, C.R.; Spencer, G.; Duffy, P.B. RCP8.5 tracks cumulative CO<sub>2</sub> emissions. *Proc. Natl. Acad. Sci. USA* **2020**, *117*, 19656–19657. [[CrossRef](#)]
25. Eames, M.; Kershaw, T.; Coley, D. The appropriate spatial resolution of future weather files for building simulation. *J. Build. Perform Simul.* **2012**, *5*, 347–358. [[CrossRef](#)]
26. De Wilde, P. The Implications of a Changing Climate for Buildings. *Build. Environ.* **2012**, *55*, 1–7. [[CrossRef](#)]
27. Kapsomenakis, J.; Kolokotsa, D.; Nikolaou, T.; Santamouris, M.; Zerefos, S.C. Forty years increase of the air ambient temperature in Greece: The impact on buildings. *Energy Convers. Manag.* **2013**, *74*, 353–365. [[CrossRef](#)]
28. D'Agostino, D.; Parker, D. How will climate alter efficiency objectives? Simulated impact of using recent versus historic European weather data for the cost-optimal design of nearly zero energy buildings (nzebs). In *E3S Web of Conferences*; EDP Sciences: Les Ulis, France, 2019; Volume 111, p. 04051. [[CrossRef](#)]



29. ASHRAE. International Weather for Energy Calculations (IWEC and IWEC2 Weather Files) Users Manual and CD-ROM. In *ASHRAE Transactions*; PART 1; American Society of Heating, Refrigerating and Air Conditioning Engineers: Atlanta, GA, USA, 2001; Volume 112, pp. 226–240.
30. Congedo, P.M.; Baglivo, C.; Zacà, I.; D’Agostino, D.; Quarta, F.; Cannoletta, A.; Marti, A.; Ostuni, V. Energy retrofit and environmental sustainability improvement of a historical farmhouse in Southern Italy. *Energy Procedia* **2017**, *133*, 367–381. [[CrossRef](#)]
31. Huang, Y.J.; Crawley, D.B. Does it Matter Which Weather Data You Use in Energy Simulations? *DOE-2 User News* **1997**, *18*, 2–12.
32. Crawley, D.B. Which Weather Data Should You Use for Energy Simulations of Commercial Buildings? In *ASHRAE Transactions*; ASHRAE: Atlanta, GA, USA, 1998; Volume 104, pp. 498–515.
33. Crawley, D.B.; Lawrie, L.K. Should I Care How Old My Climate Data Is? In Proceedings of the CIBSE ASHRAE Technical Symposium, Glasgow, UK, 16–17 April 2020.
34. Huld, T.; Paietta, E.; Zangheri, P.; Pinedo Pascua, I. Assembling Typical Meteorological Year Data Sets for Building Energy Performance Using Reanalysis and Satellite Based Data. *Atmosphere* **2018**, *9*, 53. [[CrossRef](#)]
35. D’Agostino, D.; Mazzarella, L. What is a Nearly zero energy building? Overview, implementation and comparison of definitions. *J. Build. Eng.* **2019**, *21*, 200–212. [[CrossRef](#)]
36. D’Agostino, D. Assessment of the progress towards the establishment of definitions of Nearly Zero Energy Buildings (NZEBs) in European Member States. *J. Build. Eng.* **2015**, *1*, 20–32. [[CrossRef](#)]
37. Moazami, A.; Nik, V.M.; Carlucci, S.; Geving, S. Impacts of future weather data typology on building energy performance—Investigating long-term patterns of climate change and extreme weather conditions. *Appl. Energy* **2019**, *238*, 696–720. [[CrossRef](#)]
38. WeatherShift. 2020. Available online: <https://www.weathershift.com/> (accessed on 10 February 2022).
39. Christensen, C.; Horowitz, S.; Givler, T.; Barker, G.; Courtney, A. *BEopt: Software for Identifying Optimal Building Designs on the Path to Zero Net Energy*, NREL/CP-550-3733; National Renewable Energy Laboratory: Washington, DC, USA, 2005.
40. Corrado, V.; Ballarini, I.; Corgnati, S.P. *Building Typology Brochure, Italy; Pubblicazione Nell’ambito Del Progetto Tabula*; GmbH: Darmstadt, Germany, 2014; ISBN 978-88-8202-065-1. Available online: [https://episcopo.eu/fileadmin/tabula/public/docs/brochure/IT\\_TABULA\\_TypologyBrochure\\_POLITO.pdf](https://episcopo.eu/fileadmin/tabula/public/docs/brochure/IT_TABULA_TypologyBrochure_POLITO.pdf) (accessed on 14 April 2022).
41. Attia, S.; Gratia, E.; De Herde, A.; Hensen, J. Simulation-based decision support tool for early stages of zero-energy building design. *Energy Build.* **2012**, *49*, 2–15. [[CrossRef](#)]
42. Tang, L.; Chen, C.; Tang, S.; Wu, Z.; Trofimova, P. Building Information Modeling and Building Performance Optimization. *Encycl. Sustain. Technol.* **2017**, 311–320. [[CrossRef](#)]
43. Wright, J.A.; Loosemore, H.A.; Farmani, R. Optimization of building thermal design and control by multi-criterion genetic algorithm. *Energy Build.* **2002**, *34*, 959–972. [[CrossRef](#)]
44. UNI EN 15459. *Energy Performance of Buildings, Economic Evaluation Procedure for Energy Systems in Buildings*; CEN: Brussels, Belgium, 2008.
45. Feist, W.; Pfluger, R.; Kaufmann, B.; Schnieders, J.; Kah, O. *Passivhaus Projektierungs Paket 2004*; Passivhaus Institut Darmstadt: Darmstadt, Germany, 2004.
46. Lu, Y.; Wang, S.; Yan, C.; Huang, Z. Robust optimal design of renewable energy system in nearly/net zero energy buildings under uncertainties. *Appl. Energy* **2017**, *187*, 62–71. [[CrossRef](#)]
47. Congedo, P.M.; Lorusso, C.; De Giorgi, M.G.; Marti, R.; D’Agostino, D. Horizontal air-ground heat exchanger performance and humidity simulation by computational fluid dynamic analysis. *Energies* **2016**, *9*, 930. [[CrossRef](#)]
48. Eurostat, Final Energy Consumption by Sector. 2019. Available online: [http://epp.eurostat.ec.europa.eu/portal/page/portal/statistics/search\\_database](http://epp.eurostat.ec.europa.eu/portal/page/portal/statistics/search_database) (accessed on 7 February 2022).
49. EC. Directorate-General for Economic and Financial Affairs European Economic Forecast. Available online: [http://ec.europa.eu/economy\\_finance/eu/forecasts/2015\\_spring\\_forecast\\_en.htm](http://ec.europa.eu/economy_finance/eu/forecasts/2015_spring_forecast_en.htm) (accessed on 22 February 2022).
50. Burch, J.; Christensen, C. Towards Development of an Algorithm to Predict Mains Water Temperature. In Proceedings of the 2007 American Solar Energy Society (ASES) Annual Conference, Cleveland, OH, USA, 8–12 July 2007.
51. Zacà, I.; D’Agostino, D.; Congedo, P.M.; Baglivo, C. Data of cost-optimality and technical solutions for high energy performance buildings in warm climate. *Data Brief* **2015**, *4*, 222–225. [[CrossRef](#)]
52. D’Agostino, D.; Cuniberti, B.; Bertoldi, P. Energy consumption and efficiency technology measures in European non-residential buildings. *Energy Build.* **2017**, *153*, 72–86. [[CrossRef](#)]
53. D’Agostino, D.; Parker, D.; Melià, P.; Dotelli, G. Data on roof renovation and photovoltaic energy production including energy storage in existing residential buildings. *Data Brief* **2022**, *41*, 107874. [[CrossRef](#)] [[PubMed](#)]
54. D’Agostino, D.; Tzeiranaki, S.T.; Zangheri, P.; Bertoldi, P. Data on nearly zero energy buildings (NZEBs) projects and best practices in Europe. *Data Brief* **2021**, *39*, 107641. [[CrossRef](#)] [[PubMed](#)]
55. D’Agostino, D.; Parker, D.; Melià, P. Environmental and economic data on energy efficiency measures for residential buildings. *Data Brief* **2020**, *28*, 104905. [[CrossRef](#)]
56. D’Agostino, D.; Mazzarella, L. Data on energy consumption and Nearly zero energy buildings (NZEBs) in Europe. *Data Brief* **2018**, *21*, 2470–2474. [[CrossRef](#)]
57. D’Agostino, D.; Tzeiranaki, S.T.; Zangheri, P.; Bertoldi, P. Assessing Nearly Zero Energy Buildings (NZEBs) development in Europe. *Energy Strategy Rev.* **2021**, *36*, 100680. [[CrossRef](#)]

58. Congedo, P.M.; Baglivo, C.; Zacà, I.; D'Agostino, D. High performance solutions and data for nZEBs offices located in warm climates. *Data Brief* **2015**, *5*, 502–505. [[CrossRef](#)]
59. D'Agostino, D.; Parker, D.; Melià, P.; Dotelli, G. Optimizing photovoltaic electric generation and roof insulation in existing residential buildings. *Energy Build.* **2022**, *255*, 111652. [[CrossRef](#)]
60. D'Agostino, D.; Cuniberti, B.; Bertoldi, P. Data on European non-residential buildings. *Data Brief* **2017**, *14*, 759–762. [[CrossRef](#)] [[PubMed](#)]
61. D'Agostino, D.; Zacà, I.; Baglivo, C.; Congedo, P.M. Economic and thermal evaluation of different uses of an existing structure in a warm climate. *Energies* **2017**, *10*, 658. [[CrossRef](#)]
62. D'Agostino, D.; Cuniberti, B.; Maschio, I. Criteria and structure of a harmonised data collection for NZEBs retrofit buildings in Europe. *Energy Procedia* **2017**, *140*, 170–181. [[CrossRef](#)]